Acta Montanistica Slovaca
ISSN 1335-1788
actamont.tuke.sk

Determination of carbonate minerals with different Mg content in limestone and dolomite by electron microprobe analysis

Katarzyna STANIENDA-PILECKI[1], Anna CZECH[2] and Jacek MAZUR[2]*

Authors' affiliations and addresses:
[1]Silesian University of Technology, Faculty of Mining, Safety Engineering and Industrial Automation, Department of Applied Geology
Akademicka 2 Street, 44-100 Gliwice, Poland
e-mail: Katarzyna.Stanienda-Pilecki@polsl.pl

[2]Łukasiewicz Research Network – Institute of Non-Ferrous Metals, Sowińskiego 5 Street, 44-100 Gliwice, Poland
e-mail: Anna.Czech@imn.lukasiewicz.gov.pl
e-mail: Jacek.Mazur@imn.lukasiewicz.gov.pl

***Correspondence:**
Katarzyna Stanienda-Pilecki, Silesian University of Technology, Faculty of Mining, Safety Engineering and Industrial Automation, Department of Applied Geology
Akademicka 2 Street, 44-100 Gliwice, Poland
tel.: +48 322371026;
fax: +48 32 2372290
e-mail: Katarzyna.Stnienda-Pilecki@polsl.pl

How to cite this article:
Stanienda-Pilecki, K., Czech, A. and Mazur, J., (2025), Determination of carbonate minerals with different Mg content in limestone and dolomite by electron microprobe analysis, *Acta Montanistica Slovaca,* Volume 30 (4), 1133-1150

DOI:
https://doi.org/10.46544/AMS.v30i4.20

Abstract
The results of the identification of carbonate minerals with different magnesium content present in Triassic limestones and dolomites using electron microprobe analysis. The following carbonate phases were identified: low-magnesium calcite, high-magnesium calcite, proto-dolomite, ordered dolomite, and dehuntite in samples from the Lower Muschelkalk formations: Gogolin Unit, Dziewkowice (Terebratula) Unit, and Karchowice Unit, and the Upper Muschelkalk: Tarnowice Unit. They are deposits of the Polish part of the Germanic Basin. The results allowed the calculation of the chemical formulae of the identified carbonate phases. High-Mg calcite has a higher Mg content than low-Mg calcite but lower than typical for proto-dolomite. Proto-dolomite has a lower content of Mg in comparison to the stoichiometric value for dolomite, which is typical for ordered dolomite. The identified huntite phase, because of reduced content of Mg, was named as de-huntite. The diagenetic process – dehuntization – was probably responsible for the reduced Mg content in this phase. The results of the research are the source of new data connected with the mineral composition of Triassic limestones and dolomites of the South-West part of Poland. The data provides complete information on the mineral phases of carbonate rocks of the European Germanic Basin.

Keywords
Electron microprobe, low magnesium calcite, high magnesium calcite, proto-dolomite, ordered dolomite, de-huntite

Introduction

The purpose of the study was to determine carbonates with varying Mg content using Electron Microprobe Analysis (microprobe measurements, EPMA). EPMA has already been used in previous studies as one of the methods used to characterize the structural-textural properties of carbonate rocks and their mineral and geochemical composition. The detailed development of this problem has become important due to the significant results of previous studies. Magnesium is a part form the calcium main component of: low magnesium (low-Mg) calcite, high magnesium (high-Mg) calcite, proto-dolomite, ordered dolomite, and huntite. The advantage of analysis in micro-areas is the detailed measurement of individual elements at points of the samples. This is very important when measuring Ca and Mg in carbonate phases, where the variation in the content of these elements is small. It was significant in the determination of carbonate phases with different Mg contents in Triassic limestones and dolomites of the Polish part of the Germanic Basin.

These minerals formed the Lower Muschelkalk (Middle Triassic) limestones of Opole Silesia (Stanienda, 2005, 2006, 2011, 2013 a and b, 2014, 2016 a and b, Stanienda-Pilecki, 2017, 2018, 2019, 2021, 2023; Stanienda-Pilecki & Jendruś, 2024) and the Upper Muschelkalk (Middle Triassic) dolomites of Upper Silesia (Stanienda-Pilecki, 2023; Stanienda-Pilecki & Jendruś, 2024; Szulc, 1990, 2000, 2008; Szulc & Becker, 2007). These rocks are part of the sediments of the eastern part of the epicontinental European Germanic Basin. It was an intracratonic sea basin located in various countries of central Europe. (Szulc, 1990, 2000, 2008; Szulc & Becker, 2007). In the Lower Muschelkalk limestones of the Opole-Silesian region, variable carbonate phases with different magnesium contents are present in the sediments of the Gogolin, Górażdże, Dziewkowice (Terebratula), and Karchowice units. The names of the units are the regional names of towns. Differentiation of carbonate phases rich in Mg content was also observed in the Upper Silesian Muschelkalk dolomites in sediments of the Tarnowice Unit (Stanienda-Pilecki, 2023; Stanienda-Pilecki & Jendruś, 2024; Szulc, 1990, 2000, 2008; Szulc & Becker, 2007). Carbonate phases with different Mg contents – low-Mg calcite, high-Mg calcite, proto-dolomite, ordered dolomite, and huntite – have been identified in the Lower Muschelkalk limestones of Opole Silesia. However, low-Mg calcite is the main component of the limestone. High-Mg calcite and dolomite phases are common, and huntite sometimes occurs. However, it can be said that high-magnesium calcite and huntite are not typical minerals for Triassic sediments. It is known and has been confirmed in various studies that high-Mg calcite, such as aragonite, is an unstable carbonate phase. These two phases are not preserved in older geological sediments such as the Triassic, but are transformed into low-Mg calcite during the early stage of diagenesis (eogenetic stage) (Stanienda, 2005, 2006, 2011, 2013a and b, 2014, 2016a and b, Stanienda-Pilecki, 2017, 2018, 2019, 2021, 2023; Stanienda-Pilecki & Jendruś, 2024). Huntite could be found in different types of rocks, including magmatic, sedimentary, and metamorphic. However, the results of studies of sedimentary deposits show that huntite usually occurs in the deposits of the vadose zone (Deelman, 2011).

Minerals such as calcite phases (low-Mg calcite) ($CaCO_3$) and high-Mg calcite ($CaMgCO_3$), dolomite phases – proto-dolomite ($(Ca_{0.6}, Mg_{0.4})(CO_3)_2$) and ordered dolomite ($(Ca_{0.5}, Mg_{0.5})(CO_3)_2$) and huntite $CaMg_3[CO_3]_4$ are main components of limestones and dolomites of different geological formations, including Triassic. It is very important to determine the proper content of Ca and Mg in carbonate minerals to define the conditions of the sedimentation environment of the analyzed rocks and diagenetic processes that influenced their final petrographic structure. One of the best methods for differentiating the phase composition of carbonates is Electron probe microanalysis (X-Ray microprobe analysis – EPMA) for the determination of elements in solid materials (Lane & Dalton, 1994; McGee & Keil, 2001; Sweatman & Long, 1969; Zhang et al., 2019; Yang & Jiang, 2012; Zhao et al., 2015; Zhang & Yang, 2016). It sometimes provides more detailed data than X-Ray Diffraction (XRD), Fourier Transform Infrared (FTIR), or other methods used for determining the phase composition of rocks, especially when there are mineral phases with slightly different elemental content.

Studies of carbonate minerals with different Mg contents are important for determining the environmental conditions of carbonate formation and diagenesis in the Germanic Basin research area. It is also important for analyzing the stability and solubility of mineral phases (Stanienda, 2005, 2006, 2011, 2013a and b, 2014, 2016a and b, Stanienda-Pilecki, 2017, 2018, 2019, 2021, 2023; Stanienda-Pilecki & Jendruś, 2024). The main source of magnesium is seawater and sometimes freshwater. However, weathering land carbonate or silicate rocks could also deliver some of Mg. Magnesium, after reaching a shelf zone in sea water, usually forms dolomite phases and sometimes high-Mg calcite (Mackenzie & Andersson, 2013; Morse & Mackenzie, 1990; Morse et al., 2006The stability of carbonate minerals, including magnesium ions, is affected by the different cation sizes of Ca and Mg. The length of the ionic radius and the strength of the ionic bonds are also important. It is known that the strength of the ionic bond between two calcium ions is greater than the strength of the ionic bond between calcium and magnesium because the cationic size of Mg is smaller than that of Ca (Bertram et al., 1991; Boggs, 2010; Böttcher et al., 1997; Böttcher & Dietzel, 2010). Therefore, carbonate phases rich in Mg (for instance, high-Mg calcites) are characterised by weaker stability than "pure" calcite. This is not the case for ordered, stoichiometric dolomite and huntite, where Mg is not a substituent but a major constituent of these minerals (Ahn et al. 1996; Atay & Çelik, 2010; Dollase & Reeder, 1986; Graf & Goldsmith, 1982; Kralj et al, 2004; Nash et al., 2011; Paquette & Reeder, 1990). Due to its instability compared to low magnesium calcite, high Mg calcite can lose its Mg over time and become low Mg calcite (Ahn et al. 1996; Althoff, 1977; Böttcher et al., 1997; Böttcher & Dietzel, 2010). Exposure

to Mg-rich pore waters enables high magnesium calcite to acquire additional magnesium ions and transform into dolomite (Boggs, 2010). Compared to low magnesium calcite and aragonite, calcite containing 1.9 mol% $MgCO_3$ is stable at temperatures between 25 and 64ºC. At temperatures greater than 42°C (up to 60°C), high magnesium calcite, which has the content of $MgCO_3$ up to 15 mol%, is usually stable compared with low magnesium calcite (Bertram et al., 1991). The solubility of calcite phases is also caused by the substitution of Mg. With increasing $MgCO_3$, the solubility increases (Morse et al., 1990). In many natural low-temperature environments (Böttcher et al., 1997), high magnesium calcite is common, containing up to 40% $MgCO_3$ (Zahng et al., 2010). Dolomite phases and huntite are stable carbonate phases. Magnesium is not a substitute for calcium in these minerals (Stanienda, 2013a and b, 2016a). It builds together with Ca, in appropriate proportions, these carbonates. Analysing the formation of dolomite is necessary to know that it depends on the following factors: Mg/Ca ratio, temperature, CO_2 content, and reaction time. It was studied in different research projects (Mackenzie & Andersson, 2013; Morse & Mackenzie, 1990; Morse et al., 2006; Tucker & Wright, 1990). Proto-dolomite is usually formed during sediment compaction and early stages of diagenesis (eogenetic stage). This carbonate phase is poorly ordered and non-stoichiometric, though it often forms euhedral, rhombohedral in shape crystals (Boggs, 2010; Morse & Mackenzie, 1990; Tucker & Wright, 1990). Ordered dolomite is typical, stoichiometric in chemical composition, dolomite (13.18% of Mg, 46.13% of $MgCO_3$). This carbonate phase is generally formed in magnesium-rich water environments during advanced stages of diagenesis - the mesogenetic stage, including neomorphic processes (Mackenzie & Andersson, 2013; Morse & Mackenzie, 1990; Morse et al., 2006; Tucker & Wright, 1990). Huntite could be formed by the following processes: hydrothermal processes, weathering of dolomite, and transformation of magnesium calcite in a high-temperature environment. Analyzing the sedimentary formations, this carbonate phase can be found in the rocks of the vadose zone (Althoff, 1977; Atay & Çelik, 2010; Deelman, 2011; Faust, 1953; Tucker & Wright, 1990).

Material and Methods

The materials for laboratory analyses were collected during previously conducted projects. The limestone samples were taken from the Lower Muschelkalk formation in the area of Opole Silesia: in Ligota Dolna Quarry (sample LD11), in the area os Saint Anne Mountain (sample SA5), in Szymiszów Quarry (sample S2), in Tarnów Opolski Quarry (samples TO7 and TO62), and in Strzelce Opolskie Quarry (samples SO14 and SO17). Dolomites of the Upper Muschelkalk formation were collected from the area of Upper Silesia in Lazarówka Quarry (sample LZ1) and the Piekary Śląskie (samples PSK2 and PSZ3) (Fig. 1).

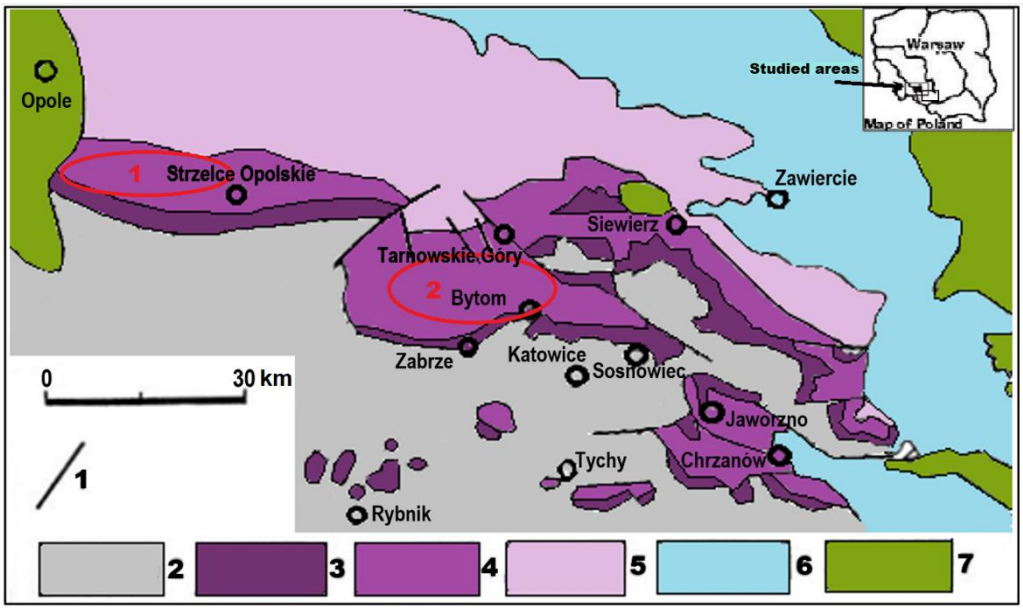

Fig. 1. A simplified geological map of the study area with the location of the sampling zones (Stanienda-Pilecki, 2023). 1- more important dislocations; 2- Paleozoic; 3- Bundsandstein; 4- Muschelkalk; 5- Upper Triassic; 6- Jurassic; 7- Cretaceous; sampling zone 1

A total of 10 samples were analysed: 7 limestones from the Lower Muschelkalk Formation and 3 dolomites from the Upper Muschelkalk Formation. The following limestones were examined: one from the Gogolin Unit – LD11, one from the Górażdże Unit – SA5, one from the Dziewkowice (Terebratula) unit – S2 (Stanienda-Pilecki, 2013a, 2023; Stanienda-Pilecki & Jendruś, 2024), and 4 from the Karchowice unit – TO7, TO62 (Stanienda, 2011), SO14 (Stanienda-Pilecki, 2013a, b, 2023), SO16 and SO17 (Stanienda-Pilecki, 2013a, 2023). Dolomite samples were taken from the Tarnowice Unit (LZ1, PSK2, PSZ3). The samples were selected based on the results of

previous projects, which involved analyzing more than one hundred samples. The results of X-ray diffraction (XRD), Fourier transform infrared spectroscopy (FTIR), X-ray fluorescence (XRF), and electron probe microanalysis (EPMA) were most relevant in the selection of samples for this study.

The studies were carried out using the techniques of X-ray microprobe analysis (Electron microprobe analysis – EPMA, with the application of a JXA-8230 X-ray microanalyser manufactured by JOEL. The measurements were done on polished sections. The accelerating voltage was 15 kV, and the electron beam current was 20nA. Quantitative analyses of the chemical composition were carried out using the wavelength dispersion (WDS) method. The size of the analyzed area, resulting from the characteristics of the electron beam and the X-ray excitation area, is of the order of 1μm^3. The maps of the element distribution were made using the energy dispersive method (EDS). The standards used were: pure metals for Fe, Mn and aluminium oxide (Al_2O_3) as a standard for aluminium and oxygen, calcium silicate ($CaSiO_3$) as a standard for silicon and calcium, iron sulphide (Fe_2S) as a standard for sulphur (for sample LZ1), diamond as a standard and magnesium oxide (MgO) as a standard for magnesium. The samples supplied were sputtered with a gold layer. They were sputtered with a carbon layer. The WDS spectrometer measurements were carried out to perform quantitative analyses in micro-areas of the samples, at selected points that differed in terms of chemical composition. The measurements were carried out on one micro-area of the samples: LD11, SA5, TO7, TO62, LZ1, PSK2, and PSZ3, and in two micro-areas of samples: S2, SO14, and SO17. In addition, an EDS method of microprobe measurement was carried out in a selected area of sample PSZ3. The chemical elements determined were Mg, Si, Al, Ca, Ba, Sr, Fe, Mn, O, and C. The total C and part of the oxygen formed carbonates. The remainder of the O formed aluminosilicates and quartz. In addition, elemental content was measured in micro-areas of samples LZ1, PSK2, and PSZ3 using the EDS method.

Results

The microprobe measurements (Electron probe microanalysis) were executed in the carbonate groundmass of the samples, at points. BSE images of selected, representative micro-areas of samples were taken. The quantitative chemical composition of the rocks at the points was determined. This method allowed for the determination of five carbonate phases: low magnesium calcite, high magnesium calcite, proto-dolomite, ordered dolomite, and de-huntite. The results were presented in Tables from 1 to 14 and Figures from 2 to 9. In tables, the calculated chemical formulas of identified minerals were presented. The names of minerals in the tables are presented in the form of abbreviations as follows: Cal- low magnesium calcite (Low-Mg calcite), Mg-Cal- high magnesium calcite (High-Mg calcite), P-Dol- proto-dolomite, O-Dol- ordered dolomite, and De-Hun- de-huntite, Hun- huntite.

Gogolin limestone from the quarry of Ligota Dolna

Only one sample, LD11, was chosen from all the rock collected in Ligota Dolna Quarry. This sample represents limestone of the Gogolin Unit. The microarea shows homogeneity in terms of chemical composition (Table 1, Figure 2). The results of measurements indicate the presence of low magnesium calcite in this sample. This carbonate phase is fair-grey in color. The contents of Mg are very low. It does not exceed the value of 0.8 %. Calculated value of MgO is below 1.4 % (Table 1). Therefore, the chemical formula for calcite determined at all measurement points was given as $(Ca_{0.99},Mg_{0.01})CO_3$.

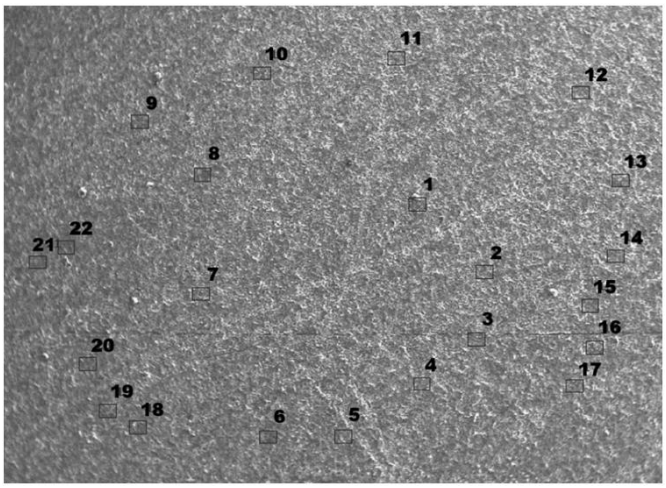

Fig. 2. BSE image of sample LD11 (Gogolin Limestone from Ligota Dolna Deposit), Magn. 500x., 1-22- points of chemical analysis.

Table 1. Microprobe chemical analyses in the micro-area of sample LD11

Point number/ Mineral chemical formula	Type of chemical element [%mass] (Fig. 2)											
	O normalized	C normalized	Mg	Si	Al	Ca	Ba	Sr	Fe	Mn	Total	MgO
1 / Cal $(Ca_{0.99},Mg_{0.01})CO_3$	54.47	9.12	0.75	2.65	0.00	29.87	0.00	0.00	3.14	0.00	100.00	1.24
2 / Cal $(Ca_{0.99},Mg_{0.01})CO_3$	54.22	9.13	0.70	1.53	0.00	31.79	0.00	0.00	2.63	0.00	100.00	1.16
3 / Cal $(Ca_{0.99},Mg_{0.01})CO_3$	54.30	9.16	0.66	3.67	0.00	30.30	0.00	0.00	1.91	0.00	100.00	1.09
4 / Cal $(Ca_{0.99},Mg_{0.01})CO_3$	54.20	9.01	0.70	2.22	0.00	30.94	0.00	0.00	2.93	0.00	100.00	1.16
5 / Cal $(Ca_{0.99},Mg_{0.01})CO_3$	54.14	9.15	0.60	1.29	0.00	33.09	0.00	0.00	1.73	0.00	100.00	0.99
6 / Cal $(Ca_{0.99},Mg_{0.01})CO_3$	54.85	9.17	0.68	2.72	0.00	29.79	0.00	0.00	2.79	0.00	100.00	1.12
7 / Cal $(Ca_{0.99},Mg_{0.01})CO_3$	53.39	9.02	0.68	1.80	0.00	32.37	0.00	0.00	2.74	0.00	100.00	1.12
8 / Cal $(Ca_{0.99},Mg_{0.01})CO_3$	54.40	9.05	0.73	2.70	0.00	30.17	0.00	0.00	2.95	0.00	100.00	1.21
9 / Cal $(Ca_{0.99},Mg_{0.01})CO_3$	54.35	8.84	0.71	2.43	0.00	30.78	0.00	0.00	2.89	0.00	100.00	1.18
10 / Cal $(Ca_{0.99},Mg_{0.01})CO_3$	54.15	9.01	0.75	2.42	0.00	30.51	0.00	0.00	3.16	0.00	100.00	1.24
11 / Cal $(Ca_{0.99},Mg_{0.01})CO_3$	54.14	9.02	0.67	2.11	0.00	31.69	0.00	0.00	2.37	0.00	100.00	1.11
12 / Cal $(Ca_{0.99},Mg_{0.01})CO_3$	54.26	8.98	0.72	2.59	0.00	30.74	0.00	0.00	3.07	0.00	100.00	1.19
13 / Cal $(Ca_{0.99},Mg_{0.01})CO_3$	54.21	8.84	0.71	2.18	0.00	31.18	0.00	0.00	2.88	0.00	100.00	1.18
14 / Cal $(Ca_{0.99},Mg_{0.01})CO_3$	53.83	9.22	0.65	2.08	0.00	31.90	0.00	0.00	2.32	0.00	100.00	1.10
15 / Cal $(Ca_{0.99},Mg_{0.01})CO_3$	54.01	9.19	0.67	2.29	0.00	30.82	0.00	0.00	3.02	0.00	100.00	1.11
16 / Cal $(Ca_{0.99},Mg_{0.01})CO_3$	54.56	9.10	0.63	2.08	0.00	30.95	0.00	0.00	2.68	0.00	100.00	1.04
17 / Cal $(Ca_{0.99},Mg_{0.01})CO_3$	53.75	9.09	0.71	2.27	0.00	31.13	0.00	0.00	3.05	0.00	100.00	1.18
18 / Cal $(Ca_{0.99},Mg_{0.01})CO_3$	54.04	9.18	0.77	1.84	0.00	31.33	0.00	0.00	2.84	0.00	100.00	1.28
19 / Cal $(Ca_{0.99},Mg_{0.01})CO_3$	54.35	8.75	0.11	2.56	0.00	31.17	0.00	0.00	3.06	0.00	100.00	0.18
20 / Cal $(Ca_{0.99},Mg_{0.01})CO_3$	51.13	9.65	0.80	2.41	0.00	33.16	0.00	0.00	2.85	0.00	100.00	1.33
21 / Cal $(Ca_{0.99},Mg_{0.01})CO_3$	54.52	9.02	0.76	3.32	0.00	28.74	0.00	0.00	3.64	0.00	100.00	1.26
22 / Cal $(Ca_{0.99},Mg_{0.01})CO_3$	54.55	8.80	0.11	2.42	0.00	31.26	0.00	0.00	2.86	0.00	100.00	0.18

Górażdże limestone from the Saint Anne Mountain outcrop

Only one sample, SA5, was chosen from all the rock collected in the Saint Anne area. This sample represents limestone of the Górażdże Beds. The micro-area shows homogeneity in terms of chemical composition (Table 2, Figure 2), as for the sample LD11 from the Gogolin Unit. Also, in this case, the results of measurements indicate the presence of low magnesium calcite in this sample. This carbonate phase is fair-grey in color. The contents of Mg are very low. It does not exceed the value of 0.26 %. Calculated value of MgO is below 0.44 % (Table 2). Therefore, the chemical formula for calcite was determined at measurement points 1 and 2 as $(Ca_{0.99},Mg_{0.01})CO_3$, whereas the formula measured at point 3 was $CaCO_3$.

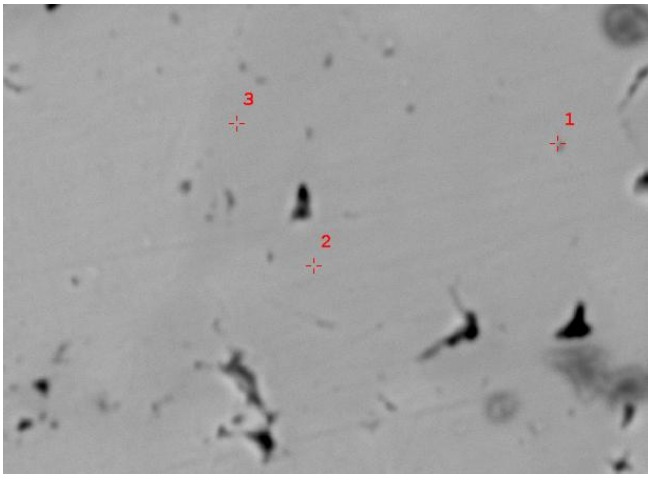

Fig. 3. BSE image of sample SA5 (Górażdże Limestone Saint Anne outcrop), Magn. 2000x., 1-3- points of chemical analysis.

Table 2. Microprobe chemical analyses in the micro-area of sample SA5

Point number/ Mineral chemical formula	Type of chemical element [%mass] (Fig. 3)											
	O normalized	C normalized	Mg	Si	Al	Ca	Ba	Sr	Fe	Mn	Total	MgO
1 / Cal $(Ca_{0.99},Mg_{0.01})CO_3$	46.06	9.69	0.26	0.00	0.01	43.84	0.01	0.06	0.04	0.03	100.00	0.43
2 / Cal $(Ca_{0.99},Mg_{0.01})CO_3$	45.12	8.94	0.23	0.00	0.00	45.63	0.00	0.00	0.07	0.01	100.00	0.38
3 / Cal $CaCO_3$	46.74	8.45	0.05	0.00	0.01	44.75	0.00	0.00	0.00	0.00	100.00	0.10

Dziewkowice limestone from the quarry of Szymiszów

Of all the rock samples from the Szymiszów quarry, only one sample – S2 – was selected for analysis. This sample represents limestone of the Dziewkowice (Terebratula) beds. Due to the heterogeneity of the sample, the measurements were carried out in two micro-areas (Tables 3 and 4, Figures 4a and 4b) (Stanienda, 2013a and b, Stanienda-Pilecki, 2023). Four carbonate phases were identified in the samples: low-Mg calcite, high-Mg calcite, ordered dolomite, and de-huntite (Tables 3 to 4, Figure 4). Calcite phases are fair grey in color, and dolomite and de-huntite are dark grey. Based on the results, chemical formulae of the identified carbonate phases were calculated. The MgO content in huntite is below the stoichiometric value for huntite (MgO – 34.25 %, Mg – 20.65 %). Some magnesium was probably removed from the crystals during the dehydration process. This carbonate phase is therefore known as de-huntite.

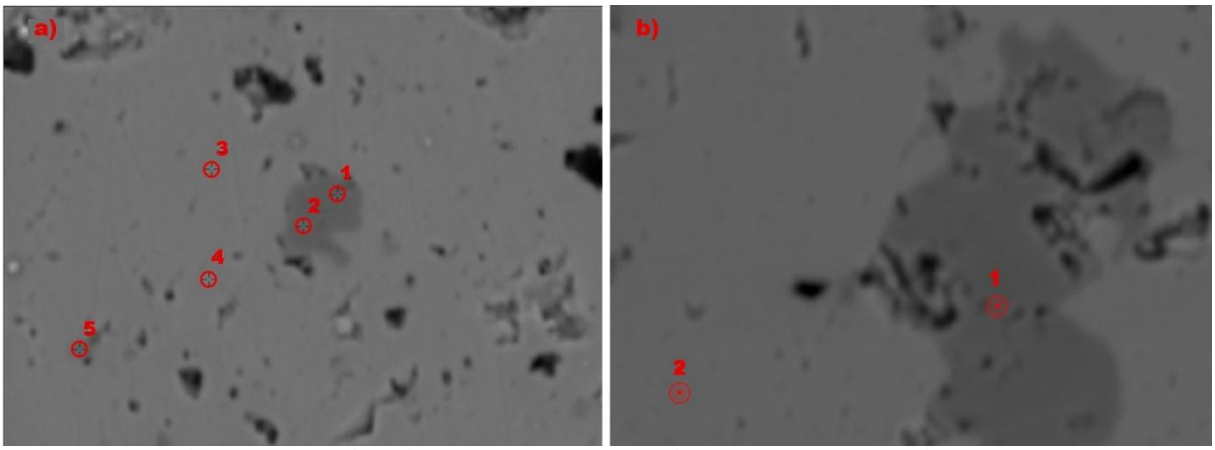

Fig. 4. BSE images of the micro-areas of sample S2 (Dziewkowice Limestone from Szymiszów Deposit), a) first micro-area, Magn. 2000x., 1-5- points of chemical analysis (Stanienda, 2013a; Stanienda-Pilecki, 2023); b) second micro-area, Magn. 2000x., 1-2- points of chemical analysis.

Table 3. Microprobe chemical analyses in the first micro-area of sample S2 (Stanienda, 2011; Stanienda-Pilecki, 2023)

Point number/ Mineral chemical formula	Type of chemical element [%mass] (Fig. 3a)											
	O normalized	C normalized	Mg	Si	Al	Ca	Ba	Sr	Fe	Mn	Total	MgO
1 / O-Dol $[Ca_{0.55},Mg_{0.45}CO_3]$	53.80	8.80	13.20	0.00	0.00	24.20	0.00	0.00	0.00	0.00	100.00	22.00
2 / Mg-Cal $(Ca_{0.66},Mg_{0.34})CO_3$	53.80	9.00	10.70	0.00	0.00	26.30	0.00	0.00	0.20	0.00	100.00	17.74
3 / Cal $(Ca_{0.99},Mg_{0.01})CO_3$	50.00	8.60	0.30	0.00	0.00	41.00	0.00	0.10	0.00	0.00	100.00	0.50
4 / Cal $(Ca_{0.99},Mg_{0.01})CO_3$	46.70	11.60	0.20	0.00	0.00	41.50	0.00	0.00	0.00	0.00	100.00	0.33
5 / Mg-Cal $(Ca_{0.77},Mg_{0.23})CO_3$	45.90	8.60	7.10	0.00	0.00	38.40	0.00	0.00	0.00	0.00	100.00	11.80

Table 4. Microprobe chemical analyses in the second micro-area of sample S2

Point number/ Mineral chemical formula	Type of chemical element [%mass] (Fig. 3b)											
	O normalized	C normalized	Mg	Si	Al	Ca	Ba	Sr	Fe	Mn	Total	MgO
1 / De-Hun $[Ca_{0.39},Mg_{0.61}CO_3]$	49.34	10.65	15.95	0.00	0.03	23.95	0.01	0.01	0.06	0.00	100.00	26.45
9 / Cal $CaCO_3$	48.25	10.95	0.33	0.00	0.01	40.41	0.00	0.02	0.01	0.02	100.00	0.55

Karchowice limestones from the quarry of Tarnów Opolski

Two limestone samples –TO7 and TO62 – selected from rock samples collected at the Tarnów Opolski quarry represent the Karchowice Beds. The results of the measurements are presented in Tables 5 and 6 and Figure 5 (Stanienda, 2011; Stanienda-Pilecki, 2023). The results of the study indicate a differentiation of the limestones in terms of the content of magnesium-enriched mineral phases. Four carbonate phases were identified in the samples: low-Mg calcite, high-Mg calcite, proto-dolomite, and ordered dolomite (Tables 5 to 6, Figure 5).

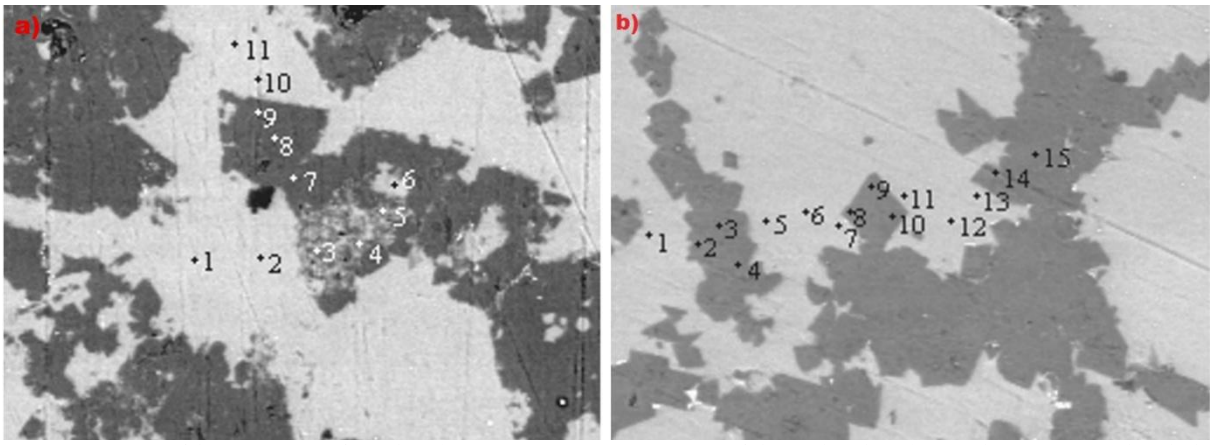

Fig. 5. BSE images of the micro-areas of samples: a) TO7 Magn. 1500x., 1-11- points of chemical analysis (Stanienda 2011; Stanienda-Pilecki, 2023); b) TO62 (Karchowice Limestones from Tarnów Opolski Deposit (Stanienda 2011; Stanienda-Pilecki, 2023).

Table 5. Microprobe chemical analyses in the micro-area of sample TO7 (Stanienda 2011; Stanienda-Pilecki, 2023)

Point number/ Mineral chemical formula	Type of chemical element [%mass] (Fig. 5a)											
	O normalized	C normalized	Mg	Si	Al	Ca	Ba	Sr	Fe	Mn	Total	MgO
1 / Cal $(Ca_{0.99},Mg_{0.01})CO_3$	52.39	4.31	0.29	0.09	0.00	42.56	0.00	0.00	0.14	0.00	100.00	0.48
2 / Cal $(Ca_{0.99},Mg_{0.01})CO_3$	49.45	8.72	0.44	0.07	0.00	41.21	0.00	0.00	0.01	0.03	100.00	0.73
3 / Mg-Cal $(Ca_{0.79},Mg_{0.21})CO_3$	48.70	7.80	6.73	0.15	0.00	36.06	0.00	0.00	0.61	0.01	100.00	11.16
4 / Mg-Cal $(Ca_{0.70},Mg_{0.30})CO_3$	49.51	9.14	9.48	0.71	0.00	30.56	0.00	0.00	0.72	0.03	100.00	15.72
5 / Mg-Cal $(Ca_{0.69},Mg_{0.31})CO_3$	50.41	8. 51	9.80	0.24	0.00	30.35	0.00	0.00	0.82	0.05	100.00	16.25
6 / Cal $(Ca_{0.95},Mg_{0.05})CO_3$	47.20	9.09	2.44	0.13	0.00	39.54	0.00	0.00	1.14	0.09	100.00	4.06
7 / O-Dol $[Ca_{0.56},Mg_{0.44}CO_3]$	52.31	7.76	13.56	0.08	0.00	25.09	0.00	0.00	0.50	0.00	100.00	22.48
8 / O-Dol $[Ca_{0.56},Mg_{0.44}CO_3]$	52.83	7.49	13.38	0.08	0.00	24.68	0.00	0.00	0.80	0.01	100.00	22.18
9 / O-Dol $[Ca_{0.56},Mg_{0.44}CO_3]$	52.64	7.70	13.67	0.12	0.00	25.06	0.00	0.00	0.76	0.13	100.00	22.50
10 / Cal $(Ca_{0.99},Mg_{0.01})CO_3$	49.67	8.43	0.35	0.04	0.00	41.60	0.00	0.00	0.13	0.02	100.00	0.58
11 / Cal $(Ca_{0.99},Mg_{0.01})CO_3$	50.01	8.80	0.32	0.07	0.00	41.01	0.00	0.00	0.03	0.01	100.00	0.53

Table 6. Microprobe chemical analyses in the micro-area of sample TO62 (Stanienda 2011; Stanienda-Pilecki, 2023)

Point number/ Mineral chemical formula	Type of chemical element [%mass] (Figure 5b)											MgO
	O normalized	C normalized	Mg	Si	Al	Ca	Ba	Sr	Fe	Mn	Total	
1 / Cal $(Ca_{0.99},Mg_{0.01})CO_3$	51.13	8.21	0.46	0.09	0.00	39.75	0.00	0.00	0.05	0.01	100.00	0.77
2 / P-Dol $[Ca_{0.61},Mg_{0.39}CO_3]$	56.13	8.66	12.34	0.11	0.00	22.40	0.00	0.00	0.47	0.04	100.00	20.57
3 / O-Dol $[Ca_{0.53},Mg_{0.47}CO_3]$	47.94	10.31	13.35	0.11	0.00	26.99	0.00	0.00	0.30	0.04	100.00	22.25
4 / PD $[Ca_{0.61},Mg_{0.39}CO_3]$	56.52	8.96	12.23	0.17	0.00	22.27	0.00	0.00	0.46	0,00	100.00	20.38
5 / Cal $(Ca_{0.99},Mg_{0.01})CO_3$	51.53	7.09	0.44	0.05	0.00	41.08	0.00	0.00	0.00	0,01	100.00	0.73
6 / Cal $(Ca_{0.99},Mg_{0.01})CO_3$	43.13	9.00	0.20	0.04	0.00	47.44	0.00	0.00	0.00	0.00	100.00	0.33
7 / Cal $(Ca_{0.99},Mg_{0.01})CO_3$	43.01	8.92	0.16	0.07	0.00	47.59	0.00	0.00	0.02	0.01	100.00	0.27
8 / P-Dol $[Ca_{0.57},Mg_{0.43}CO_3]$	55.91	8.50	12.61	0.05	0.00	22.54	0.00	0.00	0.31	0.02	100.00	21.02
9 / P-Dol $[Ca_{0.60},Mg_{0.40}CO_3]$	56.49	8.03	12.51	0.11	0.00	22.31	0.00	0.00	0.43	0.02	100.00	20.85
10 / P-Dol $[Ca_{0.60},Mg_{0.40}CO_3]$	56.66	7.32	12.53	0.09	0.00	23.02	0.00	0.00	0.12	0.00	100.00	20.88
11 / Cal $(Ca_{0.99},Mg_{0.01})CO_3$	51.69	7.25	0.21	0.05	0.00	40.66	0.00	0.00	0.06	0.01	100.00	0.35
12 / Cal $(Ca_{0.99},Mg_{0.01})CO_3$	51.93	7.69	0.12	0.06	0.00	39.88	0.00	0.00	0.05	0.05	100.00	0.20
13 / Cal $(Ca_{0.99},Mg_{0.01})CO_3$	44.14	9.50	1.08	0.09	0.00	44.94	0.00	0.00	0.12	0.00	100.00	1.80
14 / P-Dol $[Ca_{0.62},Mg_{0.38}CO_3]$	56.31	8.75	11.85	0.08	0.00	22.69	0.00	0.00	0.32	0.01	100.00	19.75
15 / P-Dol $[Ca_{0.62},Mg_{0.38}CO_3]$	56.31	8.75	11.85	0.08	0.00	22.69	0.00	0.00	0.32	0.01	100.00	19.75

In BSE images, pure calcite phases appear in light grey tones, while high-Mg calcite occasionally shows a slightly darker shade of grey compared to low-Mg calcite (Fig. 5a). The rhombohedral crystals of dolomite have a dark grey appearance (Fig. 5b). The Mg content in high-Mg calcite varies, and proto-dolomite is characterised by a lower MgO content than stoichiometric dolomite (MgO – 21.86%, Mg – 13.18%). In contrast, ordered dolomite has MgO values similar to or slightly higher than the stoichiometric values typical for dolomite. Based on the results, chemical formulae of the identified carbonate phases were calculated. They are presented in tables (Tables 5 and 6). Within the single crystals, the same carbonate phase was observed very often – ordered dolomite at points 7, 8, and 9 in the crystals of sample TO7 (Table 5, Fig. 5a) and at point 3 in the crystal of sample TO62. Proto-dolomite occurred at points 2, 4, 8, 9, 10, 14, and 15 in the crystal of sample TO62 (Table 6, Fig. 5b).

Karchowice limestones from the quarry of Strzelce Opolskie

A total of two samples were selected from all the rocks collected at the Strzelce Opolskie quarry – SO14 and SO17. These limestones represent the Karchowice Unit. Due to the diversity of these samples, the measurements were made in two micro-areas (Tables 7, 8, 9, 10, Figs 6, 7) (Stanienda, 2013a and b).

Three carbonate phases were identified in this sample, SO14: low-Mg calcite, proto-dolomite, and ordered dolomite (Tables 7, 8, Fig. 6). In the BSE image, the calcite phase is usually light grey in colour, and dolomite phases are dark grey. The results were used to calculate the chemical formulae of these phases.

The results of measurements in micro-areas of sample SO17 are presented in Tables 9 and 10 and Figure 7. Similar to sample S2 (Terebratula limestone), the MgO content in huntite is below the stoichiometric value for huntite (MgO – 34.25 %, Mg – 20.65 %). Therefore, some magnesium has probably been removed from the crystals during dehydration processes. Five carbonate phases were identified in sample SO17: low-Mg calcite, high-Mg calcite, proto-dolomite, ordered dolomite, and de-huntite. As for the SO14 and SO16 samples, the chemical formulae of the carbonate phases were also calculated for the SO17 sample. They are presented in Tables 9 and 10.

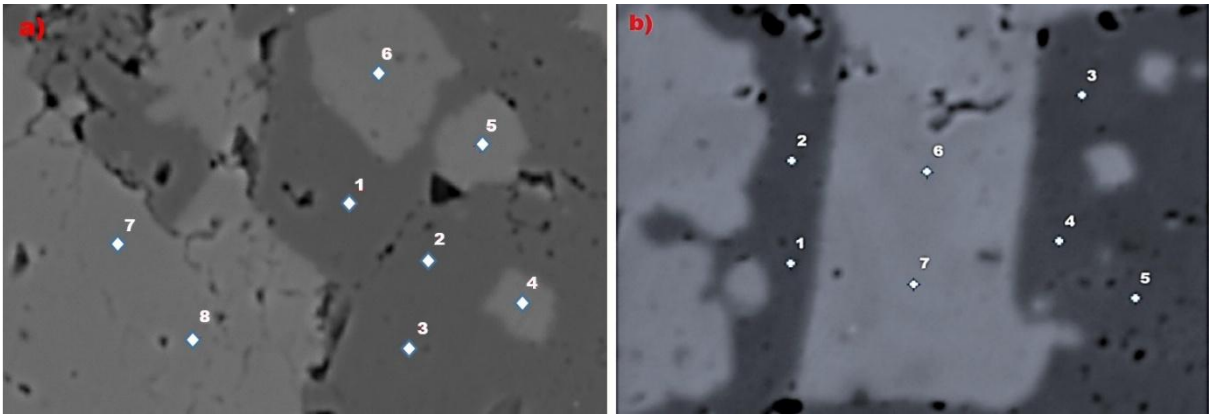

Fig. 6. BSE images of the micro-areas of samples SO14 (Stanienda, 2013a) (Karchowice Limestone from Strzelce Opolskie Deposit): a) micro-area of SO14 sample, Magn. 2000x., 1-8- points of chemical analysis; b) micro-area of SO16 sample, Magn. 2000x., 1-7- points of chemical analysis.

Table 7. Microprobe chemical analyses in the first micro-area of sample SO14 (Stanienda, 2013a)

Point number/ Mineral chemical formula	Type of chemical element [%mass] (Fig. 6a)											
	O normalized	C normalized	Mg	Si	Al	Ca	Ba	Sr	Fe	Mn	Total	MgO
1 / De-Hun [$Ca_{0.49}Mg_{0.51}CO_3$]	48.37	11.54	14.04	0.00	0.03	25.19	0.00	0.02	0.81	0.00	100.00	23.30
2 / De-Hun [$Ca_{0.49}Mg_{0.51}CO_3$]	47.32	12.90	14.01	0.00	0.02	24.78	0.00	0.00	0.97	0.00	100.00	23.23
3 / O-Dol [$Ca_{0.56}Mg_{0.44}CO_3$]	49.03	11.53	13.42	0.00	0.02	24.87	0.00	0.00	1.09	0.04	100.00	22.25
4 / De-Hun [$Ca_{0.47}Mg_{0.53}CO_3$]	46.65	12.19	14.72	0.00	0.03	24.99	0.08	0.00	1.34	0.00	100.00	24.41
5 / De-Hun [$Ca_{0.42}Mg_{0.58}CO_3$]	45.60	12.35	15.92	0.01	0.02	24.78	0.00	0.02	1.27	0.03	100.00	26.40
6 / Cal ($Ca_{0.99}Mg_{0.01}$)CO_3	42.81	14.97	0.17	0.00	0.02	41.88	0.00	0.00	0.11	0.02	100.00	0.28
7 / Cal ($Ca_{0.99}Mg_{0.01}$)CO_3	44.71	12.49	0.16	0.00	0.00	42.53	0.00	0.00	0.11	0.00	100.00	0.27
8 / Cal $CaCO_3$	43.18	12.44	0.10	0.00	0.00	44.02	0.01	0.00	0.24	0.01	100.00	0.17

Table 8. Microprobe chemical analyses in the second micro-area of sample SO14

Point number/ Mineral chemical formula	Type of chemical element [%mass] (Fig. 6b)											
	O normalized	C normalized	Mg	Si	Al	Ca	Ba	Sr	Fe	Mn	Total	MgO
1 / De-Hun [$Ca_{0.49}$,$Mg_{0.52}CO_3$]	52.72	9.09	14.36	0.05	0.06	22.49	0.00	0.00	1.19	0.04	100.00	23.81
2 / De-Hun [$Ca_{0.47}$,$Mg_{0.53}CO_3$]	50.12	11.01	14.58	0.04	0.07	22.84	0.02	0.00	1.31	0.01	100.00	24.18
3 / De-Hun [$Ca_{0.46}$,$Mg_{0.54}CO_3$]	48.42	12.73	14.93	0.00	0.02	23.01	0.00	0.01	0.83	0.05	100.00	24.80
4 / De-Hun [$Ca_{0.48}$,$Mg_{0.52}CO_3$]	48.74	12.63	14.41	0.00	0.02	22.99	0.03	0.00	1.14	0.04	100.00	24.90
5 / P-Dol [$Ca_{0.61}$,$Mg_{0.39}CO_3$]	52.67	11.42	12.17	0.11	0.16	22.20	0.00	0.06	1.18	0.03	100.00	20.20
6 / Cal ($Ca_{0.99}$,$Mg_{0.01}$)CO_3	47.87	10.98	0.22	0.13	0.07	40.57	0.00	0.00	0.14	0.02	100.00	0.36
7 / Cal ($Ca_{0.99}$,$Mg_{0.01}$)CO_3	48.85	9.35	0.10	0.00	0.00	41.56	0.00	0.00	0.09	0.05	100.00	0.17

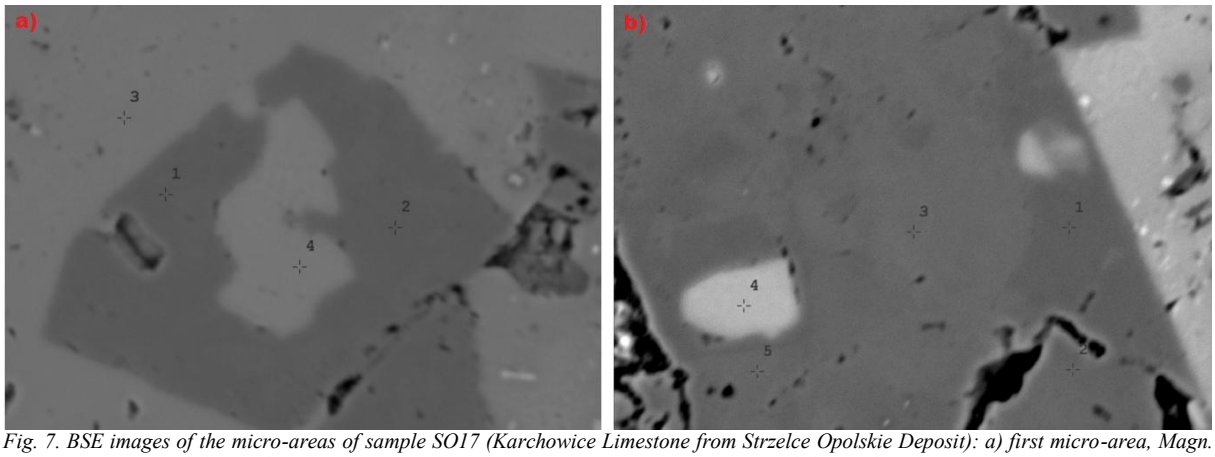

Fig. 7. BSE images of the micro-areas of sample SO17 (Karchowice Limestone from Strzelce Opolskie Deposit): a) first micro-area, Magn. 2000x., 1-5- points of chemical analysis; b) second micro-area, Magn. 2000x., 1-5- points of chemical analysis (Stanienda, 2013a).

Table 9. Microprobe chemical analyses in the first micro-area of sample SO17

Point number/ Mineral chemical formula	Type of chemical element [%mass] (Fig. 7a)											
	O normalized	C normalized	Mg	Si	Al	Ca	Ba	Sr	Fe	Mn	Total	MgO
1 / De-Hun [$Ca_{0.43}$,$Mg_{0.57}CO_3$]	50.12	9.26	15.68	0.00	0.03	24.71	0.01	0.03	0.16	0.00	100.00	26.00
2 / De-Hun t [$Ca_{0.47}$,$Mg_{0.53}CO_3$]	52.13	8.68	14.61	0.00	0.06	24.16	0.01	0.04	0.28	0.03	100.00	24.22
3 / Cal ($Ca_{0.99}$,$Mg_{0.01}$)CO	49.07	8.33	0.27	0.00	0.01	42.28	0.00	0.00	0.03	0.01	100.00	0.45
4 / Cal ($Ca_{0.99}$,$Mg_{0.01}$)CO_3	49.37	8.69	0.21	0.00	0.02	41.67	0.00	0.00	0.03	0.01	100.00	0.35

Table 10. Microprobe chemical analyses in the second micro-area of sample SO17 (Stanienda, 2013a)

Point number/ Mineral chemical formula	Type of chemical element [%mass] (Fig. 7b)											
	O normalized	C normalized	Mg	Si	Al	Ca	Ba	Sr	Fe	Mn	Total	MgO
1 / O-Dol [$Ca_{0.56}$,$Mg_{0.44}CO_3$]	52.42	9.59	13.23	0.00	0.05	24.40	0.00	0.01	0.25	0.05	100.00	22.00
2 / De-Hun [$Ca_{0.46}$,$Mg_{0.54}CO_3$]	52.52	8.04	14.81	0.00	0.16	23.48	0.00	0.01	0.97	0.01	100.00	24.56
3 / Mg-Cal ($Ca_{0.70}$,$Mg_{0.30}$)CO_3	55.38	10.17	8.71	0.00	0.02	24.19	0.04	0.00	1.47	0.02	100.00	14.44
4 / Cal ($Ca_{0.99}$,$Mg_{0.01}$)CO_3	45.86	9.15	0.13	0.00	0.00	44.76	0.00	0.03	0.05	0.02	100.00	0.22
5 / P-Dol [$Ca_{0.62}$,$Mg_{0.38}CO_3$]	53.78	10.61	11.91	0.00	0.01	22.86	0.00	0.00	0.82	0.01	100.00	19.75

Tarnowice dolomite from the quarry of Lazarówka

Only one rock sample, LZ1, was selected for examination from all the samples taken from the Lazarówka quarry near Bytom (Table 11, Fig.8). This sample is representative of the dolomite of the Tarnowice Bed.
Two carbonate phases were identified in sample LZ1: high-Mg calcite and proto-dolomite (Table 11, Figure 8). A variable Mg content was observed in the high-Mg calcite. The proto-dolomite, as in the limestone samples, is characterised by a lower MgO content than the stoichiometric one for dolomite (MgO – 21.86%, Mg – 13.18%). Moreover, pyrite was probably determined (Table 11 – point 1, Figure 8).

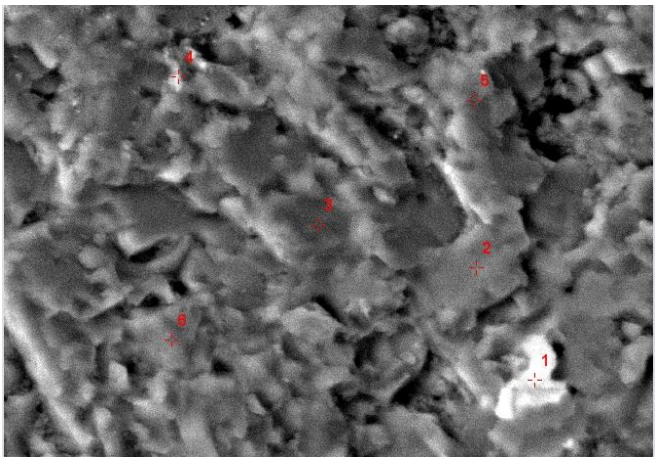

Fig. 8. BSE image of sample LZ1 (Tarnowice Dolomite from Lazarówka Quarry), Magn. 2500x., 1-6- points of chemical analysis

Table 11. Microprobe chemical analyses in the micro-area of sample LZ1

Point number/ Mineral chemical formula	Type of chemical element [%mass] (Fig. 8)												
	O normalized	C normalized	Mg	Si	Al	Ca	Ba	Sr	Fe	Mn	S	Total	MgO
1 / Pyrite FeS_2	52.10	10.58	1.20	0.74	0.05	1.47	0.00	0.00	25.44	1.05	7.37	100.00	1.99
2 / Mg-Cal $(Ca_{0.61},Mg_{0.39})CO_3$	54.19	10.93	10.37	0.00	0.07	20.96	0.00	0.00	2.87	0.60	0.01	100.00	17.19
3 / Mg-Cal $(Ca_{0.72},Mg_{028})CO_3$	55.99	12.07	7.47	0.01	0.06	21.29	0.00	0.00	2.65	0.46	0.00	100.00	12.39
4 / Mg-Cal $(Ca_{0.60},Mg_{0.40})CO_3$	53.47	11.90	10.41	0.05	0.05	21.96	0.00	0.00	1.89	0.25	0.02	100.00	17.26
5 / P-Dol [$Ca_{0.58},Mg_{0.42}CO_3$]	53.49	11.20	11.39	0.05	0.08	20.92	0.00	0.00	2.25	0.61	0.01	100.00	18.89
6 / P-Dol [$Ca_{0.58},Mg_{0.42}CO_3$]	53.44	11.29	11.71	0.01	0.11	20.69	0.00	0.00	2.17	0.56	0.02	100.00	19.42

In addition, elemental content was measured in a micro-area of sample LZ1 using the EDS method. Mesasurements were executed at three points, as well as in a 48x36µm area: C, O, Mg, Si, Al, Ca, Ba, Sr, Fe and Mn (Table 12, Fig. 9). Similar to micro-areas of some earlier studied samples, this micro-area is also dominated by a carbonate phases – ordered dolomite and the carbonate phase with an elevated magnesium content, characteristic of huntite. Due to the reduced Mg content relative to the stoichiometric one for huntite (Mg – 20.65%, MgO – 34.25%), this phase is called de-huntite.

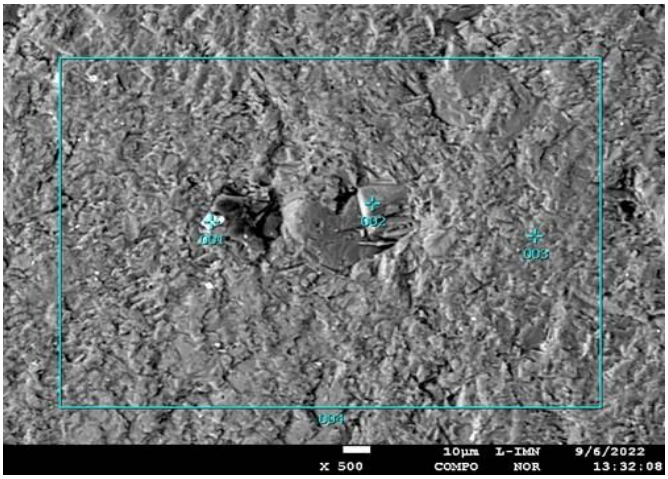

Fig.9. Composite image of the micro-area of sample LZ1 with the quantitative EDS analysis sites marked. 1-3- points of chemical analysis. A quantitative analysis of the total area (48 x 36 µm, point 4) was also performed.

Table 12. Microprobe chemical analyses of EDS measurements in the micro-area of sample PSZ3

Point number/ Mineral chemical formula	Type of chemical element [%mass] (Fig. 9b)											
	O normalized	C normalized	Mg	Si	Al	Ca	Ba	Sr	Fe	Mn	Total	MgO
1 / P-Dol [$Ca_{0.55},Mg_{0.45}CO_3$]	54.96	8.71	12.11	0.10	0.14	20.88	0.00	0.00	2.56	0.54	100.00	20.08
2 / P-Dol [$Ca_{0.55},Mg_{0.45}CO_3$]	54.96	8.71	12.11	0.10	0.14	20.88	0.00	0.00	2.56	0.54	100.00	20.08
3 / O-Dol [$Ca_{0.48},Mg_{0.52}CO_3$]	50.96	6.70	13.81	0.26	0.11	25.41	0.00	0.00	2.29	0.45	100.00	22.90
4 / Total Area P-Dol [$Ca_{0.55},Mg_{0.44}CO_3$]	52.46	8.59	11.86	0.46	0.14	23.09	0.00	0.00	2.91	0.49	100.00	19.66

Tarnowice Dolomites from Piekary Śląskie

In total, two samples were selected from all the rocks collected in the area of Piekary Śląskie – PSK2 (Table 13, Fig. 10a) and PSZ3 (Table 13, Fig. 10b). These limestones represent the Tarnowice beds.. Three carbonate phases were identified in sample PSK2: high-Mg, calcite, proto-dolomite, and ordered dolomite (Table 13, Fig. 10a). Moreover, kaolinite was determined in this sample (Table 13, Fig. 10a). Two carbonate phases were identified in sample PSZ3 using the WDS method – high-Mg calcite and proto-dolomite (Table 13, Fig. 10b). Moreover, in sample PSZ3, kaolinite was determined. A variable Mg content was observed in high-Mg calcite in both samples. The proto-dolomite, similar to sample LZ1, is characterised by a lower MgO content than the stoichiometric one for dolomite (MgO – 21.86%, Mg – 13.18%).

In addition, elemental content was measured in micro-areas of samples PSK2 and PSZ3 using the EDS method. Measurements were executed at three points, as well as in a 48x36µm area: C, O, Mg, Si, Al, Ca, Ba, Sr, Fe, and Mn (Table 15, Fig. 11). When measured using the EDS method, high-magnesium calcite was found in the micro-areas of samples PSK2 and PSZ3.

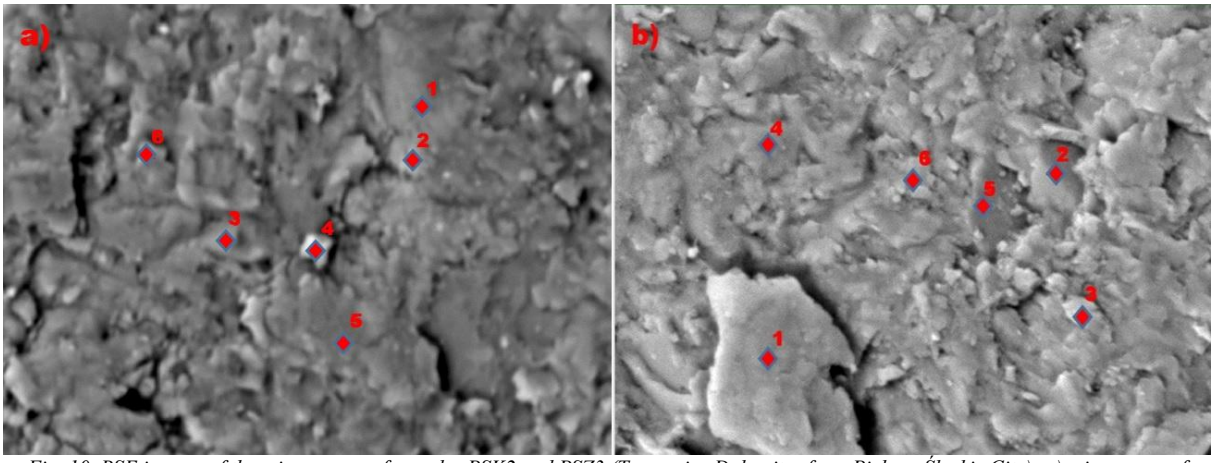

Fig. 10. BSE images of the micro-areas of samples PSK2 and PSZ3 (Tarnowice Dolomites from Piekary Śląskie City): a) micro-area of sample PSK2, Magn. 2500x., 1-6- points of chemical analysis; b) micro-area of sample PSZ3, Magn. 2500x., 1-6- points of chemical analysis.

Table 13. Microprobe chemical analyses in the second micro-area of sample PSK2

Point number/ Mineral chemical formula	Type of chemical element [%mass] (Fig. 10a)											
	O normalized	C normalized	Mg	Si	Al	Ca	Ba	Sr	Fe	Mn	Total	MgO
1 / Kaolinite ? $Al_2(Si_2O_5)(OH)_4$	51.35	10.30	1.07	17.62	13.90	2.83	0.00	0.00	2.89	0.04	100.00	1.77
2 / P-Dol $[Ca_{0.58},Mg_{0.42}CO_3]$	55.73	11.90	11.26	0.10	0.04	20.97	0.00	0.00	0.00	0.00	100.00	18.67
3 / Mg-Cal $(Ca_{0.64},Mg_{0.36})CO_3$	56.03	12.04	9.52	0.01	0.02	22.34	0.00	0.00	0.04	0.00	100.00	15.78
4 / Mg-Cal $(Ca_{0.62},Mg_{0.38})CO_3$	56.00	11.62	9.98	0.02	0.03	22.33	0.00	0.00	0.02	0.00	100.00	16.55
5 / Mg-Cal $(Ca_{0.71},Mg_{0.29})CO_3$	56.49	12.55	7.71	0.94	0.06	22.18	0.00	0.00	0.04	0.03	100.00	12.78
6 / Mg-Cal $(Ca_{0.73},Mg_{0.27})CO_3$	54.31	10.73	7.11	7.67	0.27	19.08	0.00	0.00	0.73	0.10	100.00	11.79

Table 14. Microprobe chemical analyses in the micro-area of sample PSZ3

Point number/ Mineral chemical formula	Type of chemical element [%mass] (Fig. 10b)											
	O normalized	C normalized	Mg	Si	Al	Ca	Ba	Sr	Fe	Mn	Total	MgO
1 / Mg-Cal $(Ca_{0.63},Mg_{0.37})CO_3$	55.61	11.27	9.75	2.10	0.48	20.50	0.00	0.00	0.23	0.06	100.00	16.17
2 / Mg-Cal $(Ca_{0.64},Mg_{0.36})CO_3$	51.10	11.35	9.43	6.68	0.43	20.59	0.00	0.00	0.38	0.04	100.00	15.64
3 / P-Dol $[Ca_{0.57},Mg_{0.43}CO_3]$	54.04	11.53	11.44	0.45	0.15	21.92	0.00	0.00	0.40	0.04	100.00	18.97
4 / O-Dol $[Ca_{0.51}Mg_{0.49}CO_3]$	52.37	9.99	12.98	1.84	0.16	22.47	0.00	0.00	0.14	0.03	100.00	21.52
5 / Mg-Cal $(Ca_{0.69},Mg_{0.31})CO_3$	53.75	11.55	8.23	3.07	0.35	22.79	0.00	0.00	0.21	0.06	100.00	13.65
6 / O-Dol $[Ca_{0.54},Mg_{0.46}CO_3]$	54.45	11.04	12.25	0.22	0.11	21.88	0.00	0.00	0.03	0.02	100.00	20.31

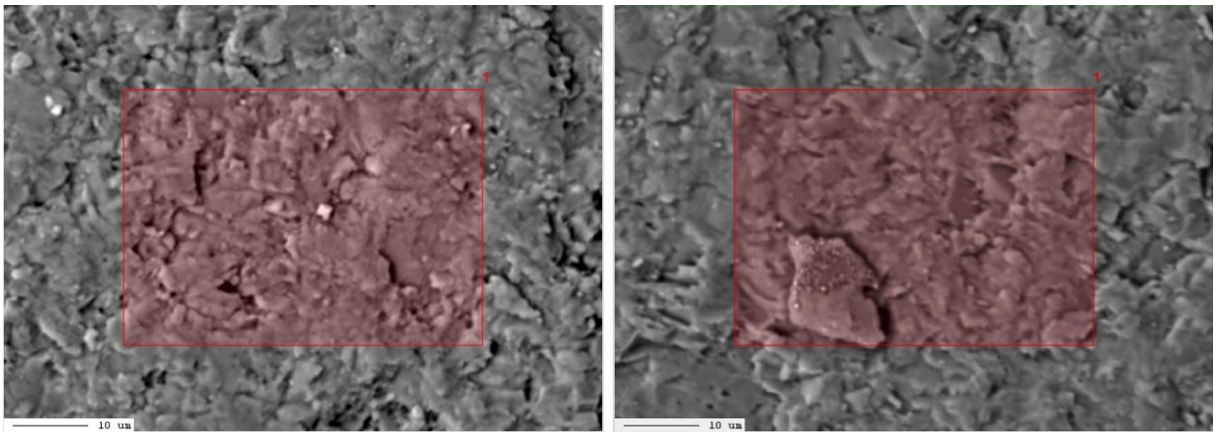

Fig.11. Composite images of samples PSK2 (a) and PSZ3 (b) with quantitative analysis spots marked, 48x36µm area.

Table 15. Microprobe chemical analyses of EDS measurements in the micro-area of sample PSZ3

Point number/ Mineral chemical formula	Type of chemical element [%mass] (Fig. 9b)											
	O normalized	C normalized	Mg	Si	Al	Ca	Ba	Sr	Fe	Mn	Total	MgO
PSK2 sample Mg-Cal ($Ca_{0.66}$,$Mg_{0.34}$)CO_3	55.96	11.38	8.89	0.75	0.25	22.48	0.00	0.00	0.29	0.00	100.00	14.74
PSZ3 sample Mg-Cal ($Ca_{0.70}$,$Mg_{0.30}$)CO_3	56.35	11.92	7.67	1.65	0.96	21.04	0.00	0.00	0.39	0.03	100.00	12.721

The results of the study indicate a differentiation of the limestones of Lower Muschelkalk formations – Gogolin, Górażdże, Dziewkowice, and Karchowice Units. Gogolin and Górażdże rocks are built of low magnesium calcite. In the samples of the Dziewkowice and Karchowice Units, the content of magnesium-enriched mineral phases is notable. Five carbonate phases were identified in the samples: low-Mg calcite, high-Mg calcite, proto-dolomite, ordered dolomite, and de-huntite (Tables 1 to 10, Figs 2 to 7). The calcite phases are light grey. In some cases, high-magnesium calcite is darker in colour than low-magnesium calcite (Fig.5a). The dolomite phases and de-huntite are dark grey. Some of the dolomite crystals are rhombohedral (Figs 4b, 6a, 7).

The Upper Muschelkalk dolomites are also differentiated by the presence of carbonate phases with varying magnesium contents. Similar to the samples from the Tarnów Opolski deposit and Strzelce Opolskie, the proto-dolomite from the Lazarówka quarry and the town of Piekary Śląskie is characterised by a lower MgO content than the stoichiometric one for dolomite. In contrast, the ordered dolomite has MgO values similar to or slightly higher than the stoichiometric values typical of dolomite (MgO – 21.86%, Mg – 13.18%). The results have been used to calculate chemical formulae for high-Mg calcite, proto-dolomite, and ordered dolomite phases. They are given in Tables 11 to 15.

Huntite phase identified in limestone samples from the Szymiszów and Strzelce Opolskie quarries and dolomite of Piekary Śląskie is characterised by a significantly lower MgO content, ranging from 23.23% (Mg – 14.01%) to 26.40% (Mg – 15.92%), than the stoichiometric value for huntite (MgO – 34.25%, Mg – 20.65%). It is likely that some magnesium was removed from the crystals of these limestones during the dehydration process. Therefore, this carbonate phase has been named de-huntite. Its chemical formula is calculated and given in Tables 4, 7, 8, 9, and 10.

Discussion

The aim of the study was to identify carbonate phases with different magnesium contents using electron microprobe analysis (X-ray spectral microanalysis, microprobe measurements). Magnesium is one of the components of five identified carbonate phases: low-Mg calcite, high-Mg calcite, proto-dolomite, ordered dolomite, and huntite phase. These carbonate phases occur in Triassic limestones of Lower Muschelkalk of Opole Silesia and Triassic dolomites of Upper Muschelkalk of Upper Silesia. X-ray microprobe analysis enables the elemental composition of selected areas of the sample to be measured. This enables the precise measurement of the elemental content at a given point. Precise magnesium measurements allow the carbonate phase at a given point to be determined. This is why this method was chosen to determine the type of carbonate phase with different Mg contents in the analysed limestones.

Occurrence of calcite phases with magnesium in Muschelkalk limestone

The analyses carried out showed that five carbonate phases were identified in samples from all the formations studied in the Lower Muschelkalk area of Opole Silesia, Poland (the Polish part of the Germanic Basin): low-Mg calcite, high-Mg calcite, proto-dolomite, ordered dolomite, and de-huntite. In the Tarnowice Formation of the Upper Silesia area (the eastern part of the Polish zone of the Germanic Basin, also known as the Upper

Muschelkalk), three carbonate phases with different magnesium (Mg) content were identified: high-Mg calcite, proto-dolomite, and ordered dolomite. A total of 10 samples were examined: LD11 represents the Gogolin Unit; SA5 represents the Górażdże Unit; S2 represents the Dziewkowice (Terebratula) Unit; and TO7, TO62, SO14, and SO17 represent the Karchowice Unit. LZ1, PSK2, and PSZ3 represent the Tarnowice Unit. In BSE images, low- and high-magnesium calcites are typically found mixed within limestone rock. These mineral phases are typically light grey in color. Occasionally, the high-magnesium calcite is darker than the low-magnesium calcite (Fig. 5a). In BSE images, dolomite and huntite phases are usually dark grey in colour. Larger, sparry, low-magnesium calcite grains often vary in size and shape (Figs 5, 6, 7). These minerals typically form either aggregates or fill veins.

Microprobe measurements indicate that the magnesium content of the low-Mg calcite phase is less than 3%. The Mg content of the high-Mg calcite phase ranges from 6.69% to 10.70%. The $MgCO_3$ content in low-Mg calcite is less than 12.16%, whereas in high-Mg calcite it ranges from 23.29% to 37.25%. Proto-dolomite is characterised by a magnesium (Mg) content ranging from 11.12% to 12.61%, whereas ordered dolomite has an Mg content ranging from 13.02% to 13.67%. The $MgCO_3$ content ranges from 38.72% to 43.91% in proto-dolomite, and from 45.34% to 47.60% in ordered dolomite. Thus, in ordered dolomite, the $MgCO_3$ value is close to the stoichiometric value for this carbonate phase. Similar values are observed for the measured Mg content within the same dolomite crystal (Tables 5, 6, Fig. 5). This indicates that the crystal contains an ordered dolomite or proto-dolomite phase. This is particularly important in the case of proto-dolomite, which is characterised by a lower than typical stoichiometric magnesium (Mg) content. If the Mg content of the same dolomite crystal were different, then it could be considered a dolomite pseudomorph. These differences can only be reliably identified through X-ray microprobe analysis. Huntite phase (named as de-huntite) was present in small amounts in all the samples examined. In BSE images, de-huntite is usually dark grey in color, similar to dolomite. The Mg content of de-huntite ranges from 14.01% to 16.18%. The $MgCO_3$ content of the identified de-huntite ranges from 48.78% to 55.44%, which is lower than the stoichiometric value of the huntite phase (69.30–72.28%). The reduction of Mg observed in de-huntite must be the result of diagenetic processes, such as dehuntitisation or calcitisation (Stanienda, 2013a, 2016a).

Structures of the crystal cell and chemical formulae of carbonate phases with magnesium

The research results presented in this article and results of previous projects (Stanienda, 2005, 2006, 2011, 2013a and b, 2014, 2016a and b, Stanienda-Pilecki, 2017, 2018, 2019, 2021, 2023; Stanienda-Pilecki & Jendruś, 2024) and also data from references allow us to determine the chemical formulas of investigated carbonate phases with magnesium. The chemical formula of the low-Mg magnesium calcite of the Lower Muschelkalk limestones can usually be shown as follows: $(Ca_{0.95},Mg_{0.05})CO_3$ or $(Ca_{0.99},Mg_{0.01})CO_3$. No major differences in Mg content were observed in the low-Mg calcite of the limestones of the studied formations. Greater differences in Mg content were observed in high-Mg calcite (high magnesium calcite / high magnesio-calcite) (Stanienda, 2011, 2013a, 2016a). The chemical formula of the high-Mg calcite of the Gogolin limestones is as follows: $Ca_{0.9}Mg_{0.1}CO_3$, whereas in the high-Mg calcite of the Górażdże limestones, the relationship is $(Ca_{0.92\text{-}0.90},Mg_{0.08\text{-}0.10})CO_3$ (Stanienda, 2013a). The chemical formula of the high-Mg calcite of the Terebratula (Dziewkowice) limestones is as follows: $(Ca_{0.77\text{-}0.66},Mg_{0.23\text{-}0.34})CO_3$, and that of the Karchowice limestones is as follows: $(Ca_{0.79\text{-}0.69},Mg_{0.21\text{-}0.31})CO_3$. The chemical formula of the high-Mg calcite of the Tarnowice dolomites is as follows: $(Ca_{0.73\text{-}0.60},Mg_{0.27\text{-}0.40})CO_3$.

The results and literature data indicate that in a single crystal cell of high-Mg calcite, made up of 14 ions, three of the ions could be Mg ions and 11 Ca ions (Stanienda, 2011, 2013a, 2016a). F. Zhang et al. (Zhang et al. 2010) found that the values of the cell parameters ao (Å) and co (Å) decrease with increasing $MgCO_3$ content in high-Mg cells. The analysis of the data obtained by F. Zhang et al. (Zhang et al. 2010) shows that it is possible to determine cell parameters on the basis of $MgCO_3$ content. When the $MgCO_3$ content is 22.7%, the cell parameters of high-Mg calcite have the following general values: a= 4.91 Å, c= 16.65 Å, and when the $MgCO_3$ content is 36.71%, the cell parameters have the following general values: a= 4.88 Å, c= 16.45 Å (Zhang et al. 2010). Substitution of magnesium in high-Mg calcite crystals makes the structure of the crystal cell different from that of the low-Mg calcite crystal. This is associated with a difference in the size of the ionic radius of Ca and the ionic radius of Mg (Table 16, Fig. 12) (Titiloye et al., 1998; Tsipursky & Buseck, 1993). Magnesium-rich carbonate minerals are characterised by a chemical formula typical of the stoichiometric value of the carbonate phase and belonging to the appropriate space group. They are as follows: low-Mg calcite – $(Ca_{1.00\text{-}0.95},Mg_{0\text{-}0.05})CO_3$, space group – scalenohedral- $R\bar{3}c$, high-Mg calcite – $(Ca_{0.92\text{-}0.74},Mg_{0.08\text{-}0.26})CO_3$, space group – rhombohedral – $R\bar{3}c$, proto-dolomite – $[Ca_{0.60\text{-}0.62},Mg_{0.40\text{-}0.38}CO_3]$, space group $R\bar{3}c$, ordered dolomite – $Ca_{0.5},Mg_{0.5}CO_3$, space group $R\bar{3}$, huntite – $[Ca_{0.25},Mg_{0.75}CO_3]$, space group R32 and magnesite – $MgCO_3$, space group $R\bar{3}c$) (Böttcher et al., 1997 a and b). According to Althoff (1977) and Paquette and Reeder (1990), the symmetry of the high magnesium calcite crystal is rhombohedral with space group $R\bar{3}c$, similar to that typical of proto-dolomite (Table 15).

Table 16. Structures of the crystal cell and chemical formulas of carbonate phases with magnesium

No	Carbonate phase name	Chemical formula	Cell parameters	Space group
1	Low-Mg calcite (Fig. 11a)	$(Ca_{1.00-0.95},Mg_{0-0.05})CO_3$	a_o= 4.989 Å, c_o= 17.062 Å	Scalenohedral- $R\bar{3}c$
2	High-Mg calcite (Fig. 11b)	Gogolin Unit- $Ca_{0.9}Mg_{0.1}CO_3$ Górażdże Unit- $(Ca_{0.92-0.90},Mg_{0.08-0.10})CO_3$ Dziewkowice Unit- $(Ca_{0.77-0.66},Mg_{0.23-0.34})CO_3$ Karchowice Unit- $(Ca_{0.79-0.69},Mg_{0.21-0.31})CO_3$ Tarnowice Unit- $(Ca_{0.73-0.60},Mg_{0.27-0.40})CO_3$	a_o= 4,941 Å, c_o= 16,854 Å	Rhombohedral- $R\bar{3}c$
3	Proto-dolomite (Fig. 11c) Ordered dolomite (Fig. 11d)	Karchowice Unit- [$Ca_{0.62-0.60},Mg_{0.38-0.40}CO_3$] Tarnowice Unit- [$Ca_{0.58-55},Mg_{0.42-45}CO_3$] Dziewkowive Unit- [$Ca_{0.55},Mg_{0.45}CO_3$] Karchowice Unit- [$Ca_{0.56-0.53},Mg_{0.44-0.47}CO_3$] Tarnowice Unit- [$Ca_{0.52},Mg_{0.48}CO_3$]	a_o= 4.842 Å, c_o= 15.95 Å	Rhombohedral- proto-dolomite- $R\bar{3}c$ Rhombohedral- ordered dolomite- $R\bar{3}$
4	Huntite (Fig. 11e(A)) De-huntite (Fig. 11e(B))	$CaMg_3[CO_3]_4$ [$Ca_{0.25},Mg_{0.75}CO_3$] Dziewkowive Unit- [$Ca_{0.39},Mg_{0.61}CO_3$] Karchowice Unit- [$Ca_{0.49-42},Mg_{0.51-58}CO_3$] Tarnowice Unit- [$Ca_{0.45-37},Mg_{0.55-63}CO_3$]	a_o= 9.5027 Å, c_o= 7.8212 Å	Trapezohedral- R32

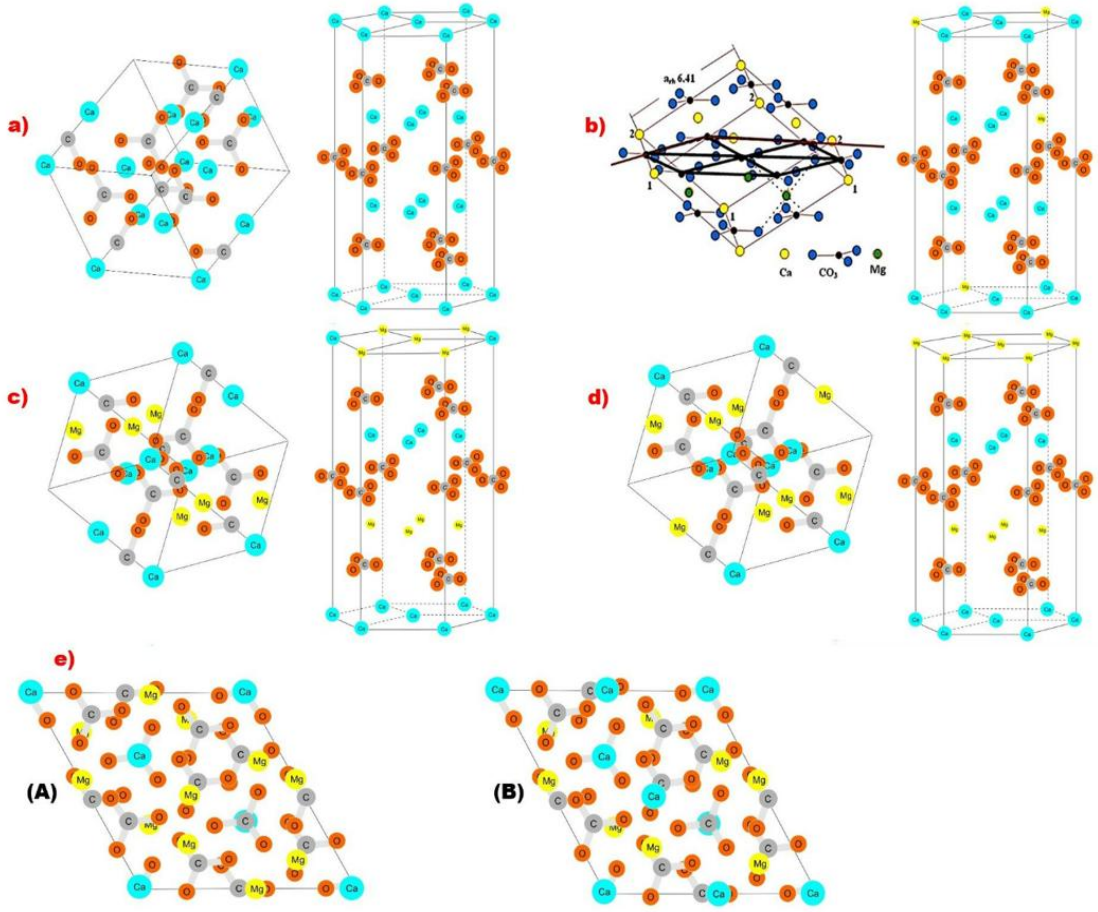

Fig. 12. Crystal structures of the carbonate phases: a) low-Mg calcite, b) high-Mg calcite, c) proto-dolomite, d) ordered dolomite, e) (A) stoichiometric huntite, (B) de-huntite (Stanienda-Pilecki, 2023).

The results of the research showed that the Triassic carbonate rocks of the Polish part of the Germanic Basin (Opole Silesia) contain a mineral that could be treated as modified huntite – magnesium and calcium carbonate with the chemical formula $CaMg_3[CO_3]_4$ (Stanienda, 2013a and b, 2016a; Stanienda-Pilecki, 2023). Due to the reduced Mg content, this carbonate phase was named de-huntite (Table 16, Fig. 12e(B)). The Mg content of the huntite phase can be shown by the following chemical formula: $Ca_{0.25},Mg_{0.75}CO_3$. According to the results of the study, the huntite of the lower Muschelkalk limestones of the Polish part of the Germanic Basin has a lower value of $MgCO_3$ (50.20% to 57.98%) than is typical for this carbonate phase, which varies from 69.30% to 72.28% of $MgCO_3$. The chemical formula of de-huntite, calculated based on the research results, can be proved as follows: $[Ca_{0.49-0.37},Mg_{0.51-0.63}CO_3]$. The reduction of Mg in this mineral can be an effect of diagenetic processes – dehuntization (calcitisation?) (Stanienda, 2013a and b, 2016a; Stanienda-Pilecki, 2023).

Environments of carbonate phases with magnesium formation

The results of the X-ray microprobe analysis also provide information on the formation of the limestones and the diagenetic processes that influenced the final mineral composition of these rocks. When considering the potential for carbonate formation, it is reasonable to conclude that both low-Mg and high-Mg calcite (the carbonate phase characterised by a higher Mg content than low-Mg calcite, but lower than dolomite) formed in the epicontinental Germanic Basin through direct crystallisation from seawater, alongside aragonite and dolomite phases (Stanienda, 2011, 2013a and b, 2016a; Stanienda-Pilecki, 2023). Dolomite phases were probably formed in the mixing zone of phreatic and salty seawater during the constructive diagenesis process in the early stages of dolomitisation. In this environment, two phases of dolomite could have formed: proto-dolomite and ordered dolomite. Furthermore, the presence of water with a high concentration of dissolved minerals in this zone caused the unstable carbonate phase of high-Mg calcite, originally formed in a seabed environment, to undergo fixation (Stanienda, 2011, 2013a and b, 2016a; Stanienda-Pilecki, 2023). Huntite is a specific carbonate phase that contains more magnesium than dolomite. This mineral can be found in igneous, sedimentary, and metamorphic rocks from various geological periods. It is typically formed through hydrothermal processes, the weathering of dolomite, or the transformation of magnesium calcite at high temperatures. It is found in the sediments of the vadose zone in sedimentary rocks (Deelman, 2011; Stanienda, 2011, 2013a and b, 2016a; Stanienda-Pilecki, 2023). De-huntite was identified in the studied samples and probably formed in areas of the Germanic Basin where diagenetic processes occurred alongside the addition of water from the vadose zone. This could explain this mineral's reduced magnesium content.

Conclusions

These results are important because they provide new data on the mineral composition of Triassic sediments in the study area. Previous studies have examined the general mineralogical composition of Muschelkalk rocks, as well as the sedimentation and diagenetic processes that influenced their final composition. However, these studies only marginally addressed the identification of carbonate phases differentiated by magnesium content. Only a few research methods enable the identification of these carbonate phases. The most important of these are X-ray diffraction and X-ray microprobe analysis.

According to the results, it can be said that:

1. X-ray microprobe analysis is one of the best methods for identifying mineral phases because of the point-by-point nature of the measurements.
2. The results of the measurements confirmed the presence of five carbonate phases with different magnesium contents in the rocks studied: a low-Mg calcite, a high-Mg calcite, a proto-dolomite, an ordered dolomite, and a de-huntite.
3. The chemical formulae of the carbonate phase have been calculated. They are as follows: low-Mg calcite – $(Ca_{1.00-0.95},Mg_{0-0.05})CO_3$, high-Mg calcite – $(Ca_{0.92-0.60},Mg_{0.08-0.40})CO_3$, proto-dolomite – $[Ca_{0.62-0.55},Mg_{0.38-0.45}CO_3]$, ordered dolomite – $[Ca_{0.55-0,52},M_{g0.45-48}CO_3]$ and de-huntite – $[Ca_{0.49-37},Mg_{0.51-63}CO_3]$.
4. Proto-dolomite is characterised by a lower Mg content than the typical stoichiometric value for dolomite, and ordered dolomite has a Mg content similar to the stoichiometric one.
5. According to the results, the de-huntite of the studied carbonate rocks has a lower value of $MgCO_3$ than the typical stoichiometric value of the huntite phase. Therefore, the huntite phase was renamed 'de-huntite'.
6. The reduction of Mg in the de-huntite can be an effect of diagenetic processes – dehuntization.
7. The results of the research extend the data connected with the mineral phases forming the Triassic carbonate rocks of the Polish part of the Germanic Basin.
8. It was possible to explain the coexistence of carbonate phases with different magnesium contents and the conditions in the sea basin that allowed the preservation in Triassic limestones of some carbonate phases, such as high-Mg calcite, characteristic of younger sediments.

In summary, the obtained data can be compared with information on the mineral composition of Triassic carbonate rocks found in other European countries and in other parts of the world. Additionally, the environmental conditions of sedimentation and the diagenetic processes undergone by Triassic carbonate rocks in different parts of the world can be compared. These processes have influenced the final form of the structural and textural features and the mineral composition of these rocks.

References

Ahn, D.J., Berman, A., & Charych, D. (1996). Probing the dynamics of template-directed calcite crystallization with in situ FTIR. *Journal of Physical Chemistry*, 100, 12455–12461. https://doi.org/10.1021/jp953536t

Althoff, P.L. (1977). Structural refinements of dolomite and a magnesian calcite and implications for dolomite formation in the marine environment. *American Mineralogist*, 62, 772–783. https://rruff.info/doclib/am/vol62/AM62_772.pdf

Atay, H.Y., & Çelik, E. (2010). Use of Turkish Huntite/Hydromagnesite Mineral in Plastic Materials as a Flame Retardant. *Polymer Composites*, 1691–1700. https://doi.org/10.1002/pc.20959

Bertram, M.A., Mackenzie, F.T., Bishop, F.C., & Bischoff, W.D. (1991). Influence of temperature on the stability of magnesian calcite. *American Mineralogist*, 76, 1889–1896. https://rruff.geo.arizona.edu/doclib/am/vol76/AM76_1889.pdf

Boggs, S Jr. (2010). Petrology of sedimentary rocks. 2nd Ed.; Cambridge University Press, United Kingdom, pp. 313–457. http://www.minsocam.org/ammin/AM76/AM76_ 1889.pdf

Böttcher, M.E., & Dietzel M. (2010). Metal-ion partitioning during low-temperature precipitation and dissolution of anhydrous carbonates and sulphates. *EMU Notes in Mineralogy*, 10, Chapter 4, 139–187. DOI:10.1180/EMU-notes.10.4

Böttcher, M.E., Gehlken, P.L., & Steele, F.D. (1997). Characterization of inorganic and biogenic magnesian calcites by Fourier Transform infrared spectroscopy. *Solid State Ionics*, 101-103, 1379–1385. https://doi.org/10.1016/s0167-2738(97)00235-x

Deelman, J.C. (2011) Low-temperature formation of dolomite and magnesite. http://www.jcdeelman.demon.nl/dolomite/files/13_Chapter6.pdf.

Dollase, W.A., & Reeder, R.J. (1986). Crystal structure refinement of huntite, $CaMg_3[CO_3]_4$, with X-ray powder data. *American Mineralogist* 71, 163–166. https://citeseerx.ist.psu.du/viewdoc/download?doi=10.1.1.561.927&rep=rep1&type=pdf

Faust, G.T. (1953). Huntite, $Mg_3Ca(CO_3)_4$, a new mineral. *American Mineralogist*, 38, 4–23. https://rruff-2.geo.arizona. edu/uploads/AM38_4.pdf

Graf, D.L., & Goldsmith, J.R. (1982). Some hydrothermal syntheses of dolomite and protodolomite. *Benchmark Papers in Geology*, *65*, 70–84. https://www.jstor.org/stable/30060650

Kralj, D., Kontrec, J., Brečěvć, L., Falini, G., & Nöthig-Laslo, V. (2004). Effect of Inorganic Anions on the Morphology and Structure of Magnesium Calcite- Chemistry. *A European Journal*, 10, 1647–1656. https://doi.org/10.1002/chem.200305313

Lane, S.J., & Dalton, J.A. (1994). Electron Microprobe Analysis of Geological Carbonates. *American Mineralogist*, 79(7/8), 745–749. https://msaweb.org/AmMin/AM79/AM79_745.pdf

Mackenzie, F.T., & Andersson, A.J. (2013**).** The Marine carbon system and ocean acidification during Phanerozoic Time. *Geochemical Perspectives,* 2(1). 10.7185/geochempersp.2.1

McGee, J.J., & Keil, K. (2001). Application of Electron Probe Microanalysis to the Study of Geological and Planetary Materials. *Microscopy and Microanalysis*, 7(2), 200–210.

Morse, J.W., Andersson, A.J., & Mackenzie, F.T. (2006). Initial responses of carbonate-rich shelf sediments to rising atmospheric pCO_2 and "ocean acidification": Role of high Mg-calcites. *Geochimica et Cosmochimica Acta*, 70, 5814–5830. 10.1016/j.gca.2006.08.017

Morse, J.W., & Mackenzie, F.T. (1990). *Geochemistry of sedimentary carbonates*. Elsevier, 33 (707). ISBN 0-444-8878 1-4 (Paperback). ISBN 0-444-8739 1-0 (Hardbound).

Nash, M.C., Troitzsch, U., Opdyke, B.N., Trafford, J.M., Russell, B.D., & Kline, D.I. (2011). First discovery of dolomite and magnesite in living coralline algae and its geobiological implications. *Biogeosciences*, 8, 3331–33340. https://doi.org/10.5194/bg-8-3331-2011

Paquette, J., & Reeder, R.J. (1990). Single-crystal X-ray structure refinements of two biogenic magnesian calcite crystals. *American Mineralogist*, 75, 1151–1158. https://rruff.geo.arizona.edu/doclib/am/vol75/AM75_1151.pdf

Stanienda, K. (2005). Identification of the carbonate phases in the Karchowice and Diplopora Beds (Muschelkalk Sediments) from the Lower Silesia. *Scientific Journals of Silesian University of Technology*, Mining 269*,* 149–157.

Stanienda, K. (2006). Carbonates in the Triassic rocks from the area of Tarnów Opolski". *Mineral Resources Management*, 22(3)*,* 243–251.

Stanienda, K. (2011). *Effects of dolomitization processes in the Triassic limestone of Tarnów Opolski Deposit.* Silesian University of Technology Press, Gliwice. ISBN: 978-83-7335-872-0

Stanienda, K. (2013a). Diagenesis of the Triassic limestone from the Opole Silesia in the aspect of magnesian calcite presence. Silesian University of Technology Press, Gliwice, ISBN: 978-83-7880-071-2

Stanienda, K. (2013b). Huntite in the Triassic limestones of Opolski Silesia. *Mineral Resources Management*, 9(3)*,* 79–98. Doi: 10.2478/gospo-2013-0036

Stanienda, K. (2014). Mineral phases in carbonate rocks of the Gogolin Beds from the area of Opole Silesia. *Mineral Resources Management*, 30(3), 17–42. Doi: 0.2478/gospo-2014-0026.

Stanienda, K. (2016a). Carbonate phases rich in magnesium in the Triassic limestones of the East part of the Germanic Basin. *Carbonates and Evaporites*, 31, 387–405. Doi: 10.1007/s13146-016-0297-2

Stanienda, K. (2016b). Mineral phases in carbonate rocks of the Górażdże Beds from the area of Opole Silesia. *Mineral Resources Management*, 32(3), 67–92. Doi: 10.1515/gospo-2016-0023

Stanienda-Pilecki, K. (2017). Carbonate minerals with magnesium in Triassic Terebratula limestone in the term of limestone with magnesium application as a sorbent in desulfurization of flue gases. *Archives of Mining Sciences*, 62(3), 459–482. Doi: 10.1515/amsc-2017-0035

Stanienda-Pilecki, K. (2018). Magnesium calcite in Muschelkalk limestones of the Polish part of the Germanic Basin. *Carbonates and Evaporites*, 33(4), 801–821. https://doi.org/10.1007/s13146-018-0437-y

Stanienda-Pilecki, K. (2019). The importance of Fourier-Transform Infrared Spectroscopy in the identification of carbonate phases differentiated in magnesium content. *Spectroscopy*, 34(6), 32–42. https://www.spectroscopyonline.com/view/spec0619-pilecki

Stanienda-Pilecki, K. (2021). The use of limestones built of carbonate phases with increased Mg content in processes of flue gas desulfurization. *Minerals*, 11(10), 1–21. https://www.mdpi.com/2075-163X/11/10/1044

Stanienda-Pilecki, K. (2023). Crystals structures of carbonate phases with Mg in Triassic rocks, mineral formation and transitions. *Scientific Reports*, 13(1), 18759–18759. https://doi.org/10.1038/s41598-023-46013-2

Stanienda-Pilecki K., & Jendruś R. (2024). Geochemical and Mineralogical Characteristics of Triassic Dolomites from Upper Silesia, Poland. *Minerals*, 14(4), 371. https://doi.org/10.3390/min14040371

Sweatman, T.R., & Long, J.V.P. (1969). Quantitative Electron-Probe Microanalysis of Rock-Forming Minerals. *Journal of Petrology*, 10(2), 332–379. https://doi.org/10.1093/petrology/10.2.332

Szulc, J. (1990). International Workshop- Field Seminar The Muschelkalk- Sedimentary Environments, Facies and Diagenesi*s*- Excursion Guidebook and Abstracts. Kraków- Opole, 1–32.

Szulc, J. (2000). Middle Triassic evolution of the Northern Peri-Tethys area is influenced by early opening of the Tethys Ocean. *Annales Societatis Geologorum Poloniae*, 70, 1–48. https://geojournals.pgi.gov.pl/asgp/article/view/12348/10822

Szulc, J. (2008). Triassic of the Silesia-Cracow area. Speleology Section Polish Society of Naturalists named after Copernicus. Materials of 42nd Speleological Symposium. Tarnowskie Góry, Poland 24-26.10.2008.

Szulc, J., & Becker A. (2007). International workshop on the Triassic of Southern Poland. Fieldtrip Guide, 30.

Titiloye, J.O., De Leeuw, N.H., & Parker, S.C. (1998) Atomistic simulation of the differences between calcite and dolomite surfaces. *Geochimica Et Cosmochimica Acta*, 62(15), 2637–2641. 10.1016/s0016-7037(98)00177-x

Tsipursky, S.J., Buseck, P.R. (1993). Structure of magnesian calcite from sea urchins. *American Mineralogist*, 7*8*, 775–781. http://www.minsocam.org/ammin/am78/am78_775.pdf

Tucker, M.E., & Wright, V.P. (1990). Carbonate sedimentology. Blackwell Scientific Publications, Oxford London, Edinburgh Boston Melbourne, 366–372. doi.org/10.1002/9781444314175

Yang, S.Y., & Jiang, S.Y. (2012). Chemical and Boron Isotopic Composition of Tourmaline in the Xiangshan Volcanic-Intrusive Complex, Southeast China: Evidence for Boron Mobilization and Infiltration during Magmatic-Hydrothermal Processes. *Chemical Geology*, 312/313, 177–189. https://doi.org/10.1016/j.chemgeo.2012.04.026

Yavuz, F., Kirikoğlu, M.S., & Özden, G. (2006). The occurrence and geochemistry of huntite from Neogene lacustrine sediments of the Yalvaç-Yarıkkaya Basin, Isparta, Turkey. *Neues Jahrbuch Fur Mineralogie-Abhandlungen*, *182/2*, 201–212. 10.1127/0077-7757/2006/0045.

Zahng, Y., & Dave, R.A. (2000). Influence of Mg^{2+} on the kinetics of calcite crystal morphology. *Chemical Geology*, 163(1-4), 129–138. https://doi.org/10.1016/S0009-2541(99)00097-2

Zhang, F., Xu, H., Konishi, H., & Roden, E.E. (2010). A relationship between d_{104} value and composition in the calcite-disordered dolomite solid-solution series. *American Mineralogist*, 95, 1650–1656. 10.2138/am.2010.3414

Zhang, R.X., & Yang, S.Y. (2016). A Mathematical Model for Determining Carbon Coating Thickness and Its Application in Electron Probe Microanalysis. *Microscopy and Microanalysis*, 22(6), 1374–1380. https://doi.org/10.1017/s143192761601182x

Zhang, X., Yang, S-H., & Zang, R. (2019). Effect of Beam Current and Diameter on Electron Probe Microanalysis of Carbonate Minerals. *Journal of Earth Science*, 30(4), 834–842. https://doi.org/10.1007/s12583-017-0939-x

Zhao, D.G., Zhang, Y.X., & Essene, E.J. (2015). Electron Probe Microanalysis and Microscopy: Principles and Applications in Characterization of Mineral Inclusions in Chromite from Diamond Deposit. *Ore Geology Reviews*, 65, 733–748. https://doi.org/ 10.1016/j.oregeorev.2014.09.020